DOI 10.1007/s11148-023-00743-y
Refractories and Industrial Ceramics *Vol. 63, No. 4, November, 2022*

INFLUENCE OF THE MEDIUM ON THE STRUCTURE AND PHASE COMPOSITION OF Ti–C–*x*NiCr (*x* = 10 – 40 wt.%) MIXTURES FROM COMBUSTION SYNTHESIS

M. S. Antipov,[1] P. M. Bazhin,[1,2] A. S. Konstantinov,[1] A. D. Bazhina,[1] and P. A. Stolin[1]

Translated from *Novye Ogneupory*, No. 8, pp. 19 – 24, August, 2022.

Original article submitted August 11, 2022.

Self-propagating high-temperature synthesis, a promising synthetic method, was proposed and used to synthesize Ti–C–*x*NiCr (*x* = 10 – 40 wt.%) mixtures. The influence of the synthesis medium (argon or vacuum) and the nickel-chromium content in the initial mixture on the phase composition of the synthesized materials, the crystal unit-cell constant of each phase, and the stoichiometry of the synthesized nickel-chromium compound was experimentally studied. The microstructure was studied. The average grain size of titanium carbide was calculated. It was established that the obtained material consisted of two phases, titanium carbide and nickel-chromium, and that the unit-cell constant of both titanium carbide and nichrome decreased with increasing mass fraction of binder from 10 to 30 wt.%. The unit-cell constant increased sharply for the composition Ti–C–40 wt.% NiCr. The effect of the medium during synthesis on the grain size of titanium carbide was studied using the composition Ti–C–30 wt.% NiCr as an example.

Keywords: SHS, combustion, titanium carbide, nickel-chromium, ceramic composite material.

INTRODUCTION

Construction materials that can operate at elevated wear levels and in various media are now attracting increased attention. For example, materials based on TiC with a metal binder that compensates for the high brittleness of the carbide have been called cermets and have broad applications because of their improved physicomechanical properties (hardness, microhardness, flexural and crushing strength, impact resistance, etc.) [1 – 5]. Cermets have also been used as wear-resistant, cutting, and high-temperature materials [6, 7]. Cermet powders can be used as materials for application of wear-resistant coatings [8 – 10]. Casting [11], sintering [12 – 14], isostatic hot pressing [15, 16], and selective laser sintering [17, 18] are the most well-known powder metallurgy methods for producing cermet items.

Self-propagating high-temperature synthesis (SHS) is the most common known method of producing metal-ceramic composites based on TiC with an added metal binder [19 – 24]. It consists of conducting an exothermic reaction as a combustion wave propagating through a layer to form synthesis products as compounds. The combustion of transition-metal powders in a reactive gas or their mixtures with nonmetals (carbon, boron) is an effective method for synthesizing carbides, nitrides, and carbonitrides. Cermets based on TiC have characteristically high melting points, hardness, corrosion resistance, etc. A metal binder, e.g., NiCr, Ni, Mo, etc., is added to TiC-based powders to decrease the brittleness of the resulting item and increase the adhesion upon application of protective coatings [25]. The SHS method produces powders and sinters that are then dispersed for further use. The advantages of SHS are the low energy consumption, high reaction rate, and purity and uniformity of the product obtained after one processing cycle as compared to traditional powder metallurgy, where syntheses require from 5 to 10 h. These features of SHS are due to the melting of the separate components of the starting mixture during the synthesis, which leads to self-dispersion of the reagents and improved uniformity of the reaction products.

The aim of the present work was to research the materials science of the combustion products from SHS from start-

[1] A. G. Merzhanov Institute of Structural Macrokinetics and Materials Science, Russian Academy of Sciences (ISMAS), Chernogolovka, Moscow Region, Russia.
[2] olimp@ism.ac.ru

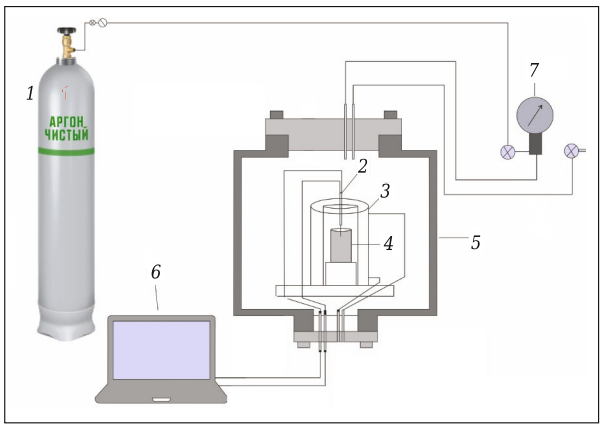

Fig. 1. Diagram of combustion in SHS mode in vacuum and in Ar: Ar tank (*1*), thermocouple (*2*), tube furnace (*3*), starting blank (*4*), reactor body (*5*), PC with data collection system (*6*), manometer (*7*).

ing Ti–C–NiCr (10 – 40 wt.%) mixtures under Ar and in a vacuum.

EXPERIMENTAL

The starting reagents were commercial powders of Ti (60 μm, 99.1%), C (1 μm, 99.1%), and NiCr (70 μm, 99.9%) calculated to form after the synthesis TiC (60 – 90 wt.%) with NiCr binder (10 – 40 wt.%) (Table 1).

The powders were mixed beforehand and dried. Then, they were pressed into cylindrical blanks of height 30 and diameter 25 mm and mass 35 g. Argon (Ar) at a pressure of 3 atm in the chamber or a vacuum of 10^{-3} mbar was used as a protective medium during the combustion in SHS mode. The cylindrical blanks had a relative density of 0.55 – 0.67 depending on the compression force of the starting powders. The range of relative density was selected to reach the maximum calculated combustion temperature in them. Figure 1 shows a diagram of the combustion in SHS mode in the protective media. Pressed blanks 4 were placed into reactor 5, where the protective medium was created. A tungsten spiral initiated the combustion from the end of the blank. After the combustion front passed, the cooled sample was removed from the chamber.

X-ray phase analysis (XPA) used an ARL X'TRA x-ray powder diffractometer with angular resolution 2θ = 20 – 80° in steps of 0.02° and a copper anode with average wavelength 1.5418 Å. XPA was performed with added Si powder to avoid instrumental error of the recorder.

The microstructure of the obtained items was studied on an LEO-1450 scanning electron microscope in combination with an INCAEnergy energy-dispersive spectroscopy microanalyzer (EDS System).

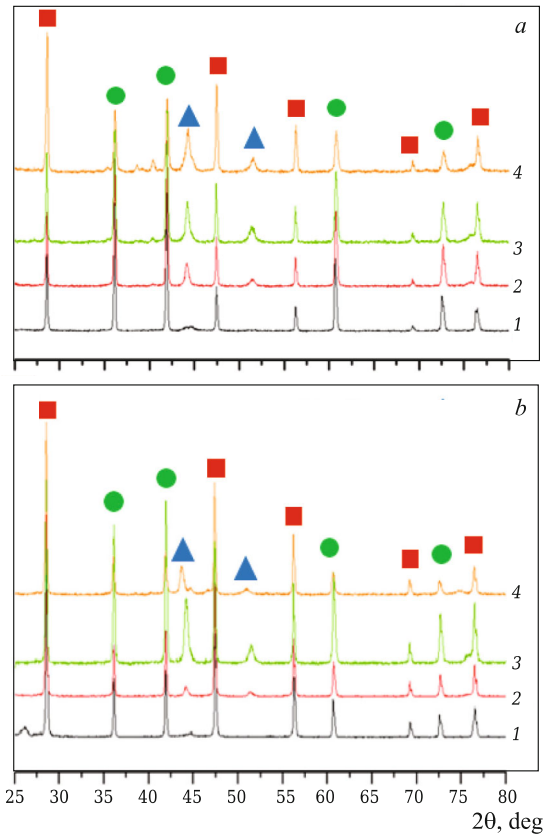

Fig. 2. XPA patterns of SHS combustion products: vacuum (*a*) and Ar (*b*); Ti–C–10 wt.% NiCr (*1*); Ti–C–20 wt.% NiCr (*2*); Ti–C–30 wt.% NiCr (*3*); Ti–C–40 wt.% NiCr (*4*); Si (■), TiC (●), NiCr (▲).

RESULTS AND DISCUSSION

The obtained samples (sinters) were further dispersed into powders of 2 μm for XPA (Fig. 2). It was found that the materials synthesized in both media consisted of the two phases TiC and NiCr. Additional strengthening phases ($Ti_{0.8}Cr_{0.2}C$ and Cr_3C_2) were not detected, e.g., like for materials prepared by SHS-extrusion [26 – 28], which in turn improved the physicomechanical properties of the obtained items. The main characteristic peaks of NiCr in the powder patterns were observed to shift to lower angles for 20 – 40 wt.% compositions and to higher angles for the

TABLE 1. Composition of Starting Components, wt.%

Composition (designation)	Ti	C	NiCr
Ti–C–10 wt.% NiCr	72	18	10
Ti–C–20 wt.% NiCr	64	16	20
Ti–C–30 wt.% NiCr	56	14	30
Ti–C–40 wt.% NiCr	48	12	40

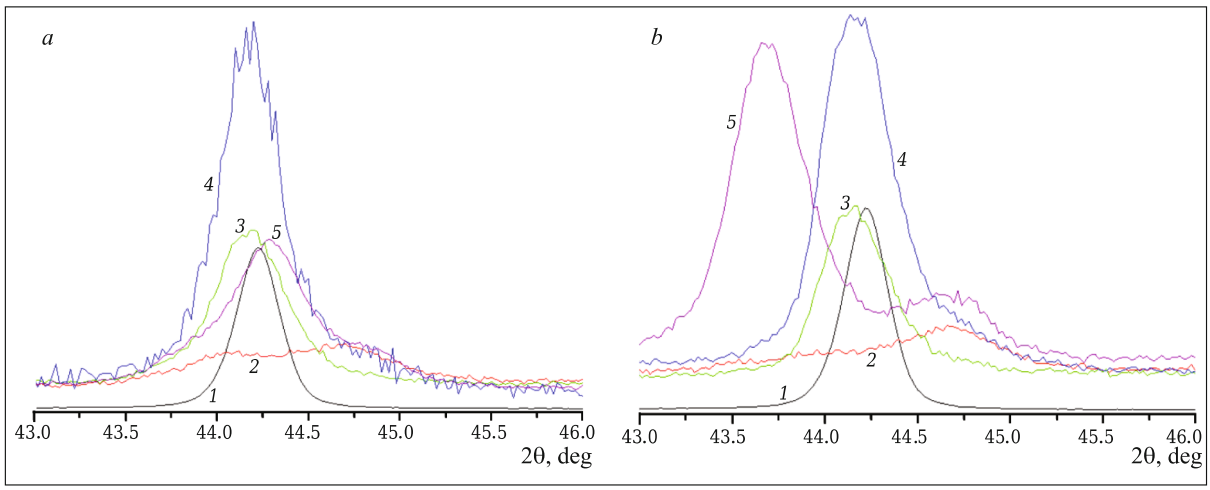

Fig. 3. Main diffraction peaks of synthesized NiCr compounds: vacuum (*a*) and Ar (*b*); starting NiCr (*1*); Ti–C–10 wt.% NiCr (*2*); Ti–C–20 wt.% NiCr (*3*); Ti–C–30 wt.% NiCr (*4*); Ti–C–40 wt.% NiCr (*5*).

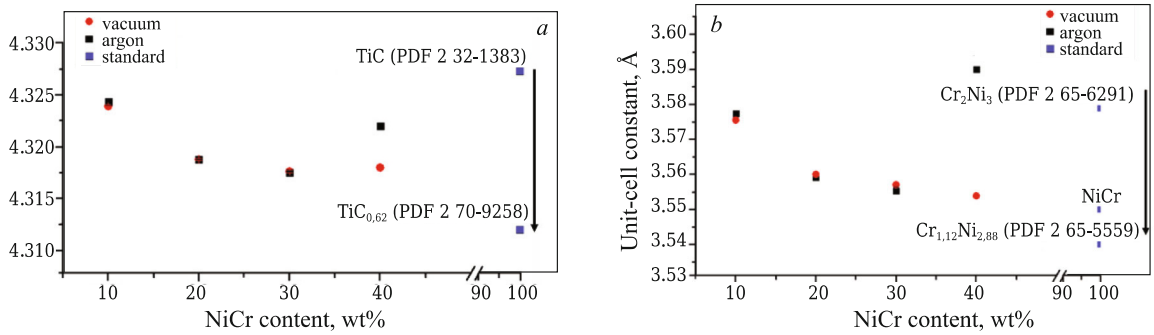

Fig. 4. Dependences of unit-cell constant *a* on NiCr content: TiC (*a*) and NiCr (*b*).

10 wt.% composition for the syntheses in Ar (Fig. 3). This shifting was not observed for the syntheses *in vacuo*. The shifting of the diffraction peaks could be explained by different combustion temperatures of the starting blanks in the studied media that affected phase and structure formation in the synthesized materials. The combustion temperature decreased if the amount of binder in the starting mixture increased because a part of the reaction heat was spent on melting the binder [29]. The greater the combustion temperature of the starting blank was, the more the diffraction peaks shifted.

The unit-cell constants of TiC and NiCr were calculated for each synthesized composition (Table 2). Regardless of the synthesis medium (Ar or vacuum), all values were similar for similar synthesis conditions. The *a* constant decreased and approached the table value for NiCr if the fraction of NiCr in the starting mixture increased. The composition Ti–C–NiCr (40 wt.%) was notable because the *a* constant of the crystal lattice increased by 0.04 Å for the material synthesized in Ar as compared to that synthesized *in vacuo*.

Dependences of unit-cell constant *a* of TiC on the NiCr content were plotted (Fig. 4). Constant *a* for standard TiC without NiCr metal binder was noted (card PDF2 32-1383) (Fig. 4*a*). Unit-cell constant *a* decreased with increasing metal-binder content in the material. All values obtained in

TABLE 2. Unit-Cell Constants

Composition	Unit-cell constant, Å	
	TiC	NiCr
Protective medium — argon		
Ti–C–10 wt.% NiCr		
Ti–C–20 wt.% NiCr	4.3183	3.5592
Ti–C–30 wt.% NiCr	4.3173	3.5554
Ti–C–40 wt.% NiCr	4.3221	3.5901
Protective medium — vacuum		
Ti–C–10 wt.% NiCr	4.3239	3.5755
Ti–C–20 wt.% NiCr	4.3187	3.5600
Ti–C–30 wt.% NiCr	4.3176	3.5571
Ti–C–40 wt.% NiCr	4.3184	3.5539

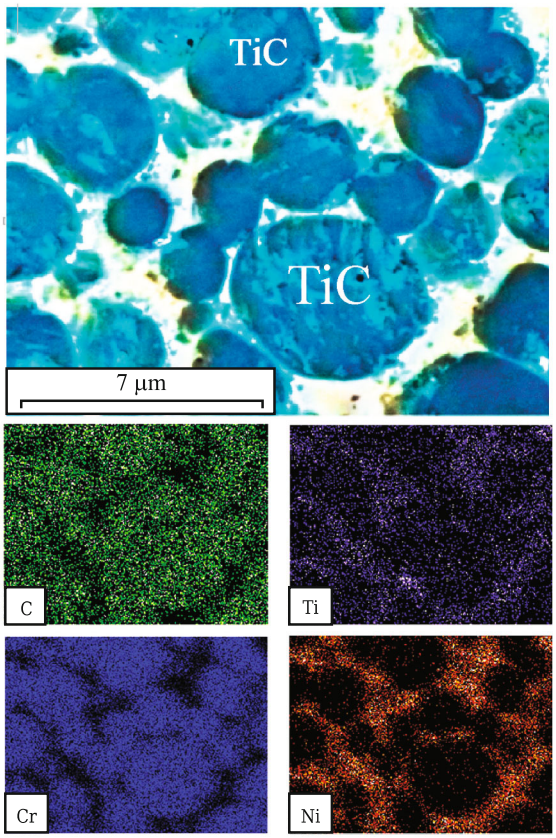

Fig. 5. EDS results in characteristic image of chemical elements.

Ar and vacuum were similar to each other although that for Ti–C–NiCr (40 wt.%) synthesized in Ar did not agree. Figure 4b shows several known compounds of Ni and Cr with various stoichiometries. Constant *a* approached the value for $TiC_{0.62}$ with increasing fraction of NiCr binder. These compounds are noted in Fig. 4 to understand to which side the stoichiometry shifted. Calculations according to Vegard's rule [30] were used to establish the stoichiometry of the formed NiCr compound from combustion in Ar or vacuum for each studied composition (Table 3). Unit-cell constant *a* decreased if the wt.% of NiCr was increased, like for the unit-cell constant for Ti–C–NiCr (40 wt.%) (Fig. 4*b*). This occurred because of various heat-transfer conditions and the combustion temperatures of the chosen compositions during the syntheses in Ar and *in vacuo*.

The structures of the synthesized materials were studied using the Ti–C–NiCr (30 wt.%) as an example (Fig. 5). EDS

TABLE 3. Nichrome Stoichiometry

NiCr content, wt.%	Stoichiometry in Ar	Stoichiometry in vacuum
10	$Ni_{60.20}Cr_{39.80}$	$Ni_{60.80}Cr_{39.20}$
20	$Ni_{65.20}Cr_{34.80}$	$Ni_{64.70}Cr_{35.30}$
30	$Ni_{65.90}Cr_{34.10}$	$Ni_{65.20}Cr_{34.80}$
40	$Ni_{56.30}Cr_{43.70}$	$Ni_{66.80}Cr_{33.20}$

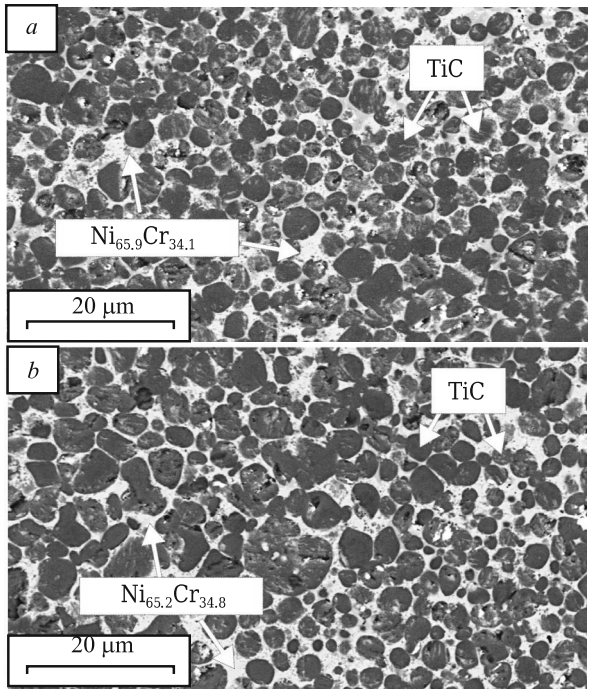

Fig. 6. SEM images of microstructure of synthesized materials: argon (*a*) and vacuum (*b*).

results in characteristic images of the chemical elements confirmed the XPA results, i.e., the material consisted of TiC grains situated in a NiCr matrix (Fig. 6). The TiC grains were round. The average TiC grain size for the materials synthesized in Ar was 2.4 μm; *in vacuo*, 1.9 μm. Heat transfer from the reaction zone was greater for the synthesis *in vacuo* as compared to that in Ar. This prevented growth of TiC grains after the combustion wave passed. Analogous results were obtained for the other compositions.

CONCLUSION

The influence of the medium on the structure and phase composition of synthesis products from combustion of Ti–C–NiCr (10 – 40 wt.%) in SHS mode was experimentally established. Unit-cell constant *a* decreased and approached the table values for TiC and NiCr as the fraction of NiCr in the starting mixture increased. Unit-cell constant *a* of NiCr increased by 0.04 Å for material synthesized in Ar as compared to that *in vacuo*, where the unit-cell constant of TiC increased by 0.0037 Å. The size of TiC grains decreased by 1.5 times for compositions synthesized *in vacuo* as compared to those synthesized in Ar because of greater heat transfer from the reaction zone.

The work was financed by grant No. MD-2909.2021.4 from the RF President for state support of young Russian scientists and doctors of science.

REFERENCES

1. R. Chandel, N. Sharma, and S. A. Bansal, "A review on recent developments of aluminum-based hybrid composites for automotive applications," *Emergent Mater.*, **4**(5), 1243 – 1257 (2021); DOI: 10.1007/s42247-021-00186-6.
2. A. R. Luts and A. D. Rybakov, "On the possibility of using various carbon forms to synthesize titanium carbide by SHS in an aluminum melt," *Sovrem. Mater., Tekh. Tekhnol.*, **5**(26), 87 – 92 (2019).
3. A. P. Amosov, A. R. Samboruk, I. V. Yatsenko, and V. V. Yatsenko, "Application of the SHS process for fabrication of ceramic-metal composite powders on the basis of titanium carbide and iron," *Vestn. Perm. Nats. Issled. Politekh. Univ. Mashinostr. Materialoved.*, **20**(4), 5 – 14 (2018); DOI: 10.15593/2224-9877/2018.4.01.
4. D. V. Aleksandrov and S. B. Malikov, "Potential of using composite materials in aviation construction," *Idei Novatsii*, **8**(3/4), 160 – 163 (2020); DOI: 10.48023/2411-7943_2020_8_3_4_160.
5. S. V. Yanyak and G. Yu. Piven?, "Experimental evaluation of the properties of solid alloys based on titanium carbide with iron-molybdenum binder," *Vestn. Vologod. Gos Univ., Ser.: Tekh. Nauki*, **1**(1), 23 – 27 (2018).
6. V. S. Svetlakov, "Advantages of using cermets as compared to solid alloys for rapid treatment of items in mechanical engineering," *Molodoi Uch.*, **49**(391), 44 – 47 (2021).
7. S. V. Yanyak and G. Yu. Piven', "Cutting properties of solid alloys based on titanium carbide with iron binder," *Vestn. Vologod. Gos. Univ., Ser.: Tekh. Nauki*, **3**(5), 78 – 81 (2019).
8. A. E. Chesnokov, A. V. Smirnov, and I. S. Batraev, "Effect of the microstructure of cermet powders on the performance characteristics of thermal spray coatings," *J. Surf. Invest.: x-ray, Synchrotron Neutron Techn.*, **13**(4), 628 – 634 (2019); DOI: 10.1134/S1027451019030248.
9. G. Bolelli, A. Colella, L. Lusvarghi, et al., "TiC-NiCr thermal spray coatings as an alternative to WC-CoCr and Cr_3C_2-NiCr," *Wear*, **450**/**451**, Art. No. 203273 (2020); DOI: 10.1016/j.wear.2020.203273.
10. A. D. Sytchenko, A. N. Sheveyko, E. A. Levashov, and Ph. V. Kiryukhantsev-Korneev, "Tribological characteristics and corrosion resistance of coatings obtained by electrospark alloying, pulsed cathodic arc evaporation, and hybrid technology using TiCNiCr and TiCNiCr–Dy_2O_3 electrodes," *Russ. J. Non-Ferrous Met.*, **61**, 325 – 331 (2020); DOI: 10.3103/S1067821220030177.
11. E. Heidari, S. M. A. Boutorabi, M. T. Honaramooz, and J. Campbell, "Ablation casting of thin-wall ductile iron," *Int. J. Metalcast.*, **16**(1), 166 – 177 (2021); DOI: 10.1007/s40962-021-00579-7.
12. Q. Zhong, H. B. Liu, L. P. Xu, et al., "An efficient method for iron ore sintering with high-bed layer: double-layer sintering," *J. Iron Steel Res. Int.*, **28**(11), 1366 – 1374 (2021); DOI: 10.1007/s42243-021-00576-4.
13. J. M. Byun, E. S. Lee, Y. J. Heo, et al., "Consolidation and properties of tungsten by spark plasma sintering and hot isostatic pressing," *Int. J. Refract. Met. Hard Mater.*, **99**, Art. No. 105602; DOI: 10.1016/j.ijrmhm.2021.105602.
14. O. V. Lapshin, E. V. Boldyreva, and V. V. Boldyrev, "Role of mixing and milling in mechanochemical synthesis (Review)," *Russ. J. Inorg. Chem.*, **66**, 433 – 453 (2021); DOI: 10.1134/S0036023621030116.
15. A. A. Khlybov, E. S. Belyaev, A. D. Ryabtsev, et al., "Hot isostatic pressing of carbide steels from chip waste of metal cutting production," *Vestn. IzhGTU im. M. T. Kalashnikova*, **23**(3), 38 – 45 (2020); DOI: 10.22213/2413-1172-2020-3-38-45.
16. S. E. Manyanin, U. Sh. Vaxidov, and K. A. Maslov, "Ways to improve the quality of products using hot isostatic pressing," *J. Adv. Res. Tech. Sci.*, **22**, 94 – 97 (2020); DOI: 10.26160/2474-5901-2020-22-94-97.
17. A. E. Nikirui, S. V. Lymar', and P. A. Drogovoz, "Time and cost of fabricating items by selective laser sintering during organization of precision production," *Sovrem. Naukoemkie Tekhnol.* **2**, 72 – 77 (2022); DOI: 10.17513/snt.39040.
18. L. P. Babentsova and I. V. Antsiferova, "Features of selective laser sintering," *Tekhnol. Mashinostr.*, **5**, 15 – 19 (2018).
19. O. B. Tomilin, E. E. Muryumin, M. V. Fadin, and S. Yu. Shchipakin, "Preparation of luminophore $CaTiO_3:Pr^{3+}$ by self-propagating high-temperature synthesis," *Russ. J. Inorg. Chem.*, **67**, 431 – 438 (2022); DOI: 10.1134/S0036023622040192.
20. V. V. Kurbatkina, E. I. Patsera, and E. A. Levashov, "Chapter 11. SHS preparation of ultrarefractory carbides," in: *Technological Combustion: Collective Monograph* [in Russian], Institute of Chemical Physics Problems of the RAS, Russ. Acad. Sci., Moscow, 2018, pp. 258 – 286; DOI: 10.31857/S9785907036383000011.
21. N. I. Radishevskaya, A. Yu. Nazarova, O. V. L'vov, et al., "Self-propagating high-temperature synthesis of $MgAl_2O_4$ spinel," *Inorg Mater.*, **56**(2), 142 – 150 (2020); DOI: 10.1134/S0020168520010112.
22. Y. Nakashima, R. Kamiya, H. Hyuga, and S. Hashimoto, "Rapid fabrication of Al_4SiC_4 using a self-propagating high-temperature synthesis method," *Ceram. Int.*, **46**(11), Part B, 19228 – 19231 (2020); DOI: 10.1016/j.ceramint.2020.04.260.
23. N. Resnina, V. Rubanik, Jr., V. Rubanik, et al., "Influence of the Ar pressure on the structure of the NiTi foams produced by self-propagating high-temperature synthesis," *Mater. Lett.*, **299**, Art. No. 130047 (2021); DOI: 10.1016/j.matlet.2021.130047.
24. A. P. Chizhikov, A. S. Konstantinov, and P. M. Bazhin, "Self-propagating high-temperature synthesis of ceramic material based on aluminum-magnesium spinel and titanium diboride," *Russ. J. Inorg. Chem.*, **66**(8), 1115 – 1120 (2021); DOI: 10.1134/S0036023621080039.
25. Yu. S. Borisov, A. L. Borisova, M. V. Kolomytsev, et al., "Protective and functional powder coatings high-velocity air plasma spraying of (Ti,Cr)C–32 wt.% Ni clad powder," *Powder Metall. Met. Ceram.*, **56**, 305 – 315 (2017); DOI: 10.1007/s11106-017-9898-0.
26. P. M. Bazhin, A. P. Chizhikov, A. M. Stolin, et al., "Long-sized rods of Al_2O_3–SiC–TiB_2 ceramic composite material obtained by SHS-extrusion: Microstructure, x-ray analysis and properties," *Ceram. Int.*, **47**(20), 28444 – 28448 (2021); DOI: 10.1016/j.ceramint.2021.06.262.
27. M. S. Antipov, A. P. Chizhikov, A. S. Konstantinov, and P. M. Bazhin, "Sintered material based on titanium carbide to increase the service life of slide gates," *Refract. Ind. Ceram.*, **62**(2), 208 – 211 (2021); DOI: 10.1007/s11148-021-00584-7.
28. P. M. Bazhin, E. V. Kostitsyna, A. M. Stolin, et al., "Nanostructured ceramic composite rods: Synthesis, properties and application," *Ceram. Int.*, **45**(7), Part A, 9297 – 9301 (2019); DOI: 10.1016/j.ceramint.2019.01.188.
29. M. S. Antipov, P. M. Bazhin, A. D. Bazhina, and A. S. Konstantinov, "Combustion temperature and relative density of ceramic-metal materials based on titanium carbide and nichrome (PC20N80) in SHS mode" [in Russian], in: *Current Solid-State Technologies: Proceedings of the XIIIth International Scientific-Innovative Youth Conference*, Tambov, Nov. 11 – 12, 2021, Tambov State Technical University, Tambov, 2021, pp. 65 – 67.
30. M. N. Magomedov, "On deviation from Vegard's rule with increasing pressure in alloys," *Inorg. Mater.*, **56**(9), 903 – 908 (2020); DOI: 10.1134/S0020168520090125.